Optical properties of synthetic porphyrins bearing or lacking an exo-five-membered ring and a keto carbonyl group on it, both of which are present in naturally occurring chlorophylls

Michio Kunieda, Emi Nakato, Hitoshi Tamiaki *

Department of Bioscience and Biotechnology, Faculty of Science and Engineering, Ritsumeikan University, Kusatsu, Shiga 525-8577, Japan

Abstract

By modifying β-octaethylporphyrin we prepared 13^1-oxo- and deoxo-porphyrins **1** and **3** possessing an exo-five-membered E-ring, which is a structural requirement of naturally occurring chlorophyllous pigments, and also 13^1-oxo- and deoxo-porphyrins **2** and **4** lacking the E-ring as reference compounds. Visible absorption spectra of 13^1-deoxo-porphyrins **3/4** bearing/lacking the E-ring and their zinc complexes showed a relatively small difference, indicating that geometry of the tetrapyrrole unit in **3** was altered by formation of the E-ring but its contribution to the visible spectrum was limited. In contrast, a spectral difference between 13^1-oxo-porphyrins **1/2** bearing/lacking the E-ring (as well as their zinc complexes) was clearly observed; fixation of 13^1-oxo group by the E-ring as in **1** resulted in its red-shifted absorption spectrum (ca. 10 nm for each band). These results indicated that introduction of the E-ring to a porphyrin macrocycle slightly affected its optical properties and that a larger effect was observed by fixation of 13^1-oxo group to a porphyrin π-conjugate system.
© 2006 Elsevier B.V. All rights reserved.

Keywords: Cyclization; Fluorescence; Photosynthesis; Porphyrinoids; Visible spectroscopy

1. Introduction

Molecular structures of naturally occurring chlorophyllous pigments utilized in the light-harvesting antennas and electron-transferring reaction centers of all photosynthetic organisms are classified by their π-conjugate systems of cyclic tetrapyrroles (porphyrin, chlorin and bacteriochlorin) and their peripheral substituent groups, as in chlorophyll(Chl)s-*a/b/c/d* and bacteriochlorophyll(BChl)s-*a/b/c/d/e/g*, and also some of their demetallated pigments, pheophytin(Phe)s and bacteriopheophytin(BPhe)s (see representative molecular structures drawn in Fig. 1) [1]. Molecular structures of natural (B)Chls are somewhat different from each other but they have many common features, one of which is the presence of a 13-keto-carbonyl group fixed on an exo-five-membered E-ring. In their biosynthetic pathways [2], the E-ring was always constructed from magnesium protoporphyrin IX monomethyl ester by cyclase, and the resulting protochlorophyllide-*a* is a common precursor of all the natural (B)Chls, so that all the photoactive (B)Chls have the E-ring as a structural motif. Some chlorophyllous pigments isolated from sediment extracts have a structural diversity including the altered E-ring, but such sedimentary pigments were generated by age-old degradation processes [3]. Thus all the photo-functionalized chlorophyllous pigments inevitably have the 13-keto-carbonyl group fixed on the E-ring to achieve robust interaction with protein scaffolds and closely packed self-aggregates in photosynthetic systems [4–6]. In addition to the structural requirement of the E-ring in chlorophyllous pigments, electronic contribution of substituents on the E-ring to the π-conjugated cyclic tetrapyrrole system is important. The 13-keto-carbonyl group in (B)Chls is fixed on the E-ring, which strongly conjugates with the skeletal π-system without any dissipation derived from its conformational rotamers as observed in the 3-carbonyl groups of Chl-*d* and BChls-*a/b*. The delocalization of the 13-C=O π-electrons into the tetrapyrrolic macrocycle is different in the presence or absence of its fixation by the E-ring, which affects their π-conjugate systems and also optical properties. Chlorin and bacteriochlorin π-conjugate systems are used in a large

---

* Corresponding author. Tel.: +81 77 566 1111; fax: +81 77 561 2659.
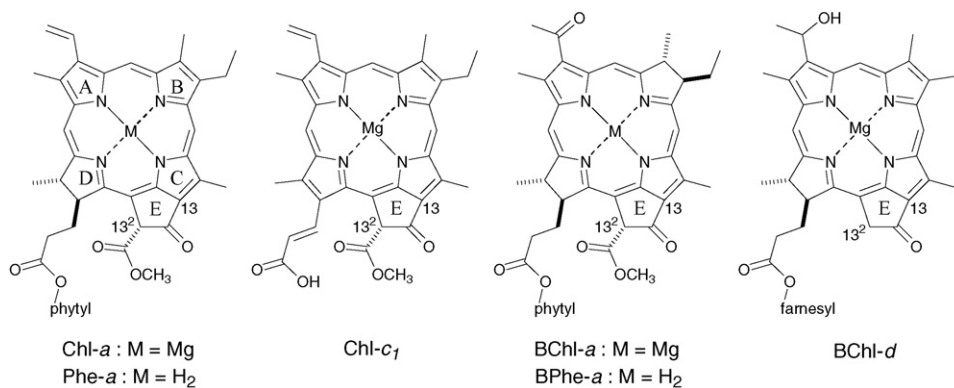 *E-mail address:* tamiaki@se.ritsumei.ac.jp (H. Tamiaki).

Fig. 1. Molecular structures of some naturally occurring chlorophyllous pigments.

portion of (B)Chls/Phes but their asymmetrical π-systems and structural diversity at the peripheral substituents complicate their optical properties; a symmetrical porphyrin π-conjugate system possessing only the same alkyl group at the other β-positions was selected for the present study to elucidate the electronic effect of a carbonyl group conformationally fixed on the E-ring.

Many synthetic studies introducing the E-ring to porphyrin macrocycle have been reported [7–18]. Typically, Lash and his colleague synthesized porphyrin **6** lacking the keto-carbonyl group on the exo-five-membered E-ring (see Scheme 1) [18] and several synthetic porphyrins bearing the expanded E-ring (six, seven and more expanded rings) [16,17], by condensation of dipyrroles. Convenient acid-catalyzed cyclization of vinyl-porphyrin **5** to **6** reported by Callot and co-workers (Scheme 1 upper) utilized another method to introduce the E-ring on porphyrin macrocycle [13]. Some porphyrins possessing a keto-carbonyl group on the exo-five-membered E-ring, similar to the molecular structures of natural (B)Chls were synthesized. Smith

and co-workers reported synthesis of porphyrin derivative **8** possessing a β-keto-ester on the E-ring by using thallium mediated photocyclization of the corresponding ring-opening porphyrin **7** (Scheme 1 lower) [8]. However, the spectral changes resulting from the fixation of keto-carbonyl group on the E-ring have not been investigated systematically.

As simple models for elucidation of the above spectral effect of the E-ring and 13-C=O in (B)Chls, we prepared four porphyrins 13^1-oxo-**1/2** and 13^1-deoxo-**3/4** bearing/lacking the E-ring, and their zinc complexes **Zn1–Zn4** (see their molecular structures drawn in Fig. 2). Since these porphyrins (**Zn**)**1–3** were prepared from octaethylporphyrin **4**, no additional substituent
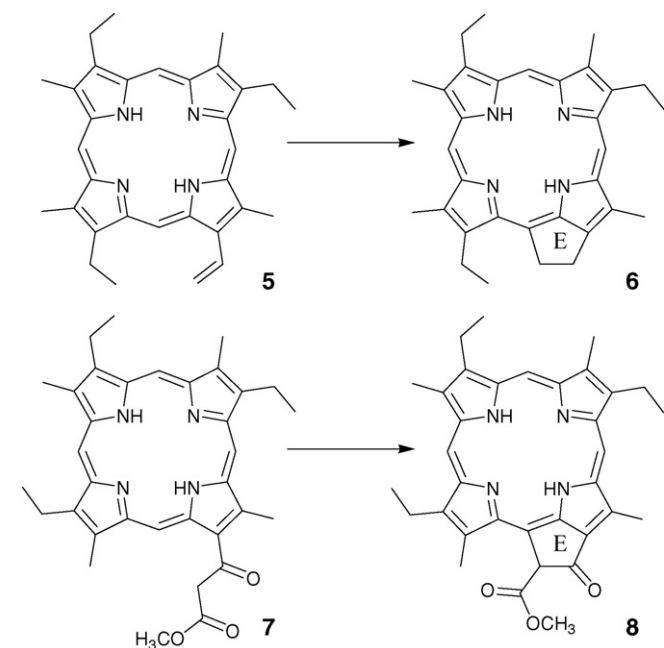
Scheme 1. Preparation of porphyrins **6** and **8** bearing an exo-five-membered E-ring reported in Refs. [8,13].
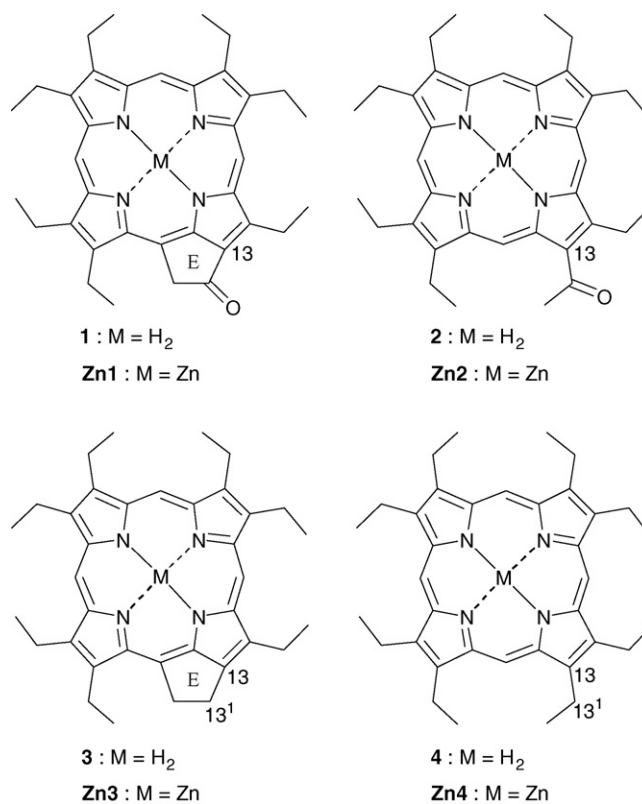

Fig. 2. Molecular structures of synthetic 13^1-oxo-porphyrins bearing the E-ring (**Zn**)**1** and lacking it (**Zn**)**2**, and their corresponding 13^1-deoxo-porphyrins (**Zn**)**3** and (**Zn**)**4**.

effects to the porphyrin π-system would be considered for their optical properties, leading to the elucidation of the optical effect between the presence and absence of the E-ring and 13-C=O. In accordance with IUPAC–IUB nomenclature for β-substituted porphyrins [19], **1** is called 3,7,8,12,13,17,18-heptaethyl-2^1,2^2-dihydro-2^1-oxocyclopenta[*at*]porphyrin (the skeletal carbon substituted by carbonyl group is labeled as the 2-position, 2^1-oxo-porphyrin), but the same β-carbon attached to the C=O moiety in naturally occurring (B)Chls and (B)Phes is labeled as the 13-position (see Fig. 1). To compare natural with synthetic porphyrinoids, in this paper, the numbering of the positions in all the synthetic compounds is used for that in the natural chlorophylls and does not follow the above nomenclature: typically 13^1-oxo-**1**.

2. Experimental

2.1. General

Visible absorption and fluorescence emission spectra were measured on Hitachi U-3500 and F-4500 spectrophotometers, respectively. ^{1}H NMR spectra in chloroform-*d* were recorded with a JEOL ECA-600 equipment; TMS was used as an internal standard. For NMR measurements of zinc complexes, 1% (v/v) pyridine-d_5 was added for their monomerization. ^{1}H–^{1}H COSY and NOESY ($\tau_m = 400$ ms) techniques were used to confirm the molecular structures. MS spectra ionized by FAB were obtained on a JEOL GCmate II spectrometer; samples were dissolved in dichloromethane (chloroform/methanol for zinc complexes) and *m*-nitrobenzyl alcohol was added as a matrix. FCC was carried out on silica gel (Merck Kieselgel 60, 9358). Dichloromethane for visible absorption and fluorescence spectra was purchased from Nacalai Tesque (Kyoto, Japan, spectroscopy grade). All procedures including syntheses and spectral measurements were performed at rt in the dark.

Octaethylporphyrin **4** was available from Tokyo Kasei Kogyo Co., Ltd. (TCI, Tokyo, Japan). 13-Acetyl-2,3,7,8,12,17,18-heptaethylporphyrin (**2**), its zinc complex **Zn2**, **Zn4**, 2,3,7,8, 12,17,18-heptaethyl-13-vinyl-porphyrin (**9**) and zinc 2,3,7,8,12, 17,18-heptaethyl-13-formyl-porphyrin (**Zn10**) were prepared according to the reported procedures [20]. 3^1,3^2-Didehydro-phytoporphyrin methyl ester (**14**) [21], its zinc complex **Zn14** [21], 3^1,3^2-didehydro-rhodoporphyrin dimethyl ester (**15**) [22] and its zinc complex **Zn15** [23] were synthesized according to the previous reports.

2.2. Synthesis of porphyrins

2.2.1. Synthesis of zinc 13-[1-hydroxy-2-(methoxycarbonyl)ethyl]porphyrin Zn11

Sodium iodide (235.6 mg), indium powder (247.2 mg) and methyl bromoacetate (700 µl) were added to a THF solution (13 ml) of **Zn10** (118.0 mg) and treated with ultra-sound for about 1.5 h at 55 °C [24]. The reaction was monitored by visible spectroscopy until the Soret band moved from 417 to 401 nm. After filtration to remove indium powder, the organic solution was diluted with water and extracted with dichloromethane. The

organic layer was washed with 4% aq. NaHCO$_3$ and water, dried over Na$_2$SO$_4$ and evaporated to dryness. Unreacted bromide and **Zn10** were removed on FCC by hexane and dichloromethane, respectively, and the desired product **Zn11** was obtained (10% diethyl ether/dichloromethane). Recrystallization from dichloromethane/hexane gave pure **Zn11** (25.6 mg, 20%); vis (CH$_2$Cl$_2$) $\lambda_{max} = 569$ (relative intensity, 0.06), 531 (0.04), 401 nm (1.00); ^{1}H NMR (CDCl$_3$) $\delta = 10.43$, 10.03, 10.02 (1H + 1H + 2H, s, *meso*-H × 4), 6.91 (1H, dd, $J = 3.5$, 10 Hz, 13-CH), 4.28–4.07 (14H, m, β-CH$_2$ × 7), 3.94 (1H, dd, $J = 10$, 17 Hz, 13^1-CH), 3.33 (1H, dd, $J = 3.5$, 17 Hz, 13^1-CH), 3.81 (3H, s, 13^2-CO$_2$CH$_3$), 1.99–1.88 (21H, m, β-CCH$_3$ × 7); MS (FAB) m/z 670.1 (M$^+$), calcd. for C$_{38}$H$_{46}$N$_4$O$_3$^{64}Zn: 670.3.

2.2.2. Synthesis of 13-[2-(methoxycarbonyl)acetyl]porphyrin 12

To a dichloromethane solution of **Zn11** (25.6 mg), *N*-methylmorpholine *N*-oxide (25.6 mg) and tetrapropylammonium perruthenate (10.0 mg) were added and stirred under nitrogen [20,25]. The reaction was monitored by visible spectroscopy until complete red-shift of the Soret band from 401 to 409 nm. After 15-min stirring, the reaction mixture was passed through a silica gel column to remove tetrapropylammonium perruthenate, and **Zn12** was separated (3% diethyl ether/dichloromethane). After evaporation, the residue was dissolved in an acetone (6 ml) and aq. 10% HCl (0.5 ml) was added to the solution and stirred for 20 min. The reaction mixture was diluted with water and extracted with dichloromethane, washed with aq. 4% NaHCO$_3$ and water, dried over Na$_2$SO$_4$, and evaporated to dryness. Recrystallization from dichloromethane/hexane gave metal-free **12** (8.6 mg, total yield of 37% from **Zn11**). The keto–enol ratio was estimated as ca. 5:6 from the integral ratio of its ^{1}H NMR peaks; vis (CH$_2$Cl$_2$) $\lambda_{max} = 629$ (rel., 0.03), 570 (0.07), 546 (0.10), 507 (0.08), 408 nm (1.00); ^{1}H NMR (CDCl$_3$) $\delta = 13.24$ (1H, s, enol-OH), 10.69, 10.17, 10.01 (1H + 1H + 2H, s, keto–*meso*-H × 4), 10.50, 10.20, 10.06 (1H + 1H + 2H, s, enol–*meso*-H × 4), 6.12 (1H, s, enol-13^1-CH), 4.76 (2H, s, keto-13^1-CH$_2$), 4.35, 4.29 (2H, q, $J = 8$ Hz, keto + enol-12-CH$_2$), 4.16–3.97 (12H, m, keto + enol-2,3,7,8,17,18-CH$_2$ × 6), 4.03 (3H, s, enol-13^2-CO$_2$CH$_3$), 3.93 (3H, s, keto-13^2-CO$_2$CH$_3$), 2.00, 1.98 (3H, t, $J = 8$ Hz keto + enol-12^1-CH$_3$), 1.93–1.87 (18H, m, keto + enol-2^1, 3^1, 7^1, 8^1, 17^1, 18^1-CH$_3$ × 6), −3.60, −3.72 (each 1H, s, NH × 2); MS (FAB) m/z 606.3 (M$^+$), calcd. for C$_{38}$H$_{46}$N$_4$O$_3$: 606.4.

2.2.3. Synthesis of 13^2-methoxycarbonyl-13^1-oxoporphyrin bearing the E-ring 13

To a dichloromethane solution (11.4 ml) of **12** (8.6 mg), a tetrahydrofuran solution (2.8 ml) of thallium(III) trifluoroacetate (17.9 mg) was added, and stirred for 10 min under an irradiation of white light (a Sumita LS-M250 metal-halide lamp) [8]. Then the reaction was quenched by 2-min treatment of SO$_2$ gas (prepared by 10% aq. H$_2$SO$_4$ and NaHSO$_3$), and the central thallium was removed by 1-min treatment of conc. HCl. The reaction mixture was diluted with dichloromethane (30 ml), washed with water three times, dried over Na$_2$SO$_4$ and evaporated to dryness. Purification by FCC (dichloromethane) and

recrystallization from dichloromethane/hexane gave desired **13** as a pure form (4.5 mg, 53%); vis (CH$_2$Cl$_2$) λ_{max} = 633 (rel., 0.06), 588 (0.12), 566 (0.13), 524 (0.10), 420 nm (1.00); ^{1}H NMR (CDCl$_3$) δ = 10.21, 9.96, 9.95 (each 1H, s, *meso*-H × 3), 7.01 (1H, s, 13^2-H), 4.11–3.95 (14H, m, β-CH$_2$ × 7), 3.81 (3H, s, 13^2-CO$_2$CH$_3$), 2.09–1.53 (21H, m, β-CCH$_3$ × 7), −2.49, −3.35 (each 1H, s, NH × 2); MS (FAB) *m/z* 604.4 (M$^+$), calcd. for C$_{38}$H$_{44}$N$_4$O$_3$: 604.3.

2.2.4. Synthesis of 13^1-oxoporphyrin bearing the E-ring 1

Porphyrin **13** (4.5 mg) was dissolved in collidine (15 ml) and refluxed for 3 h under nitrogen [22]. After evaporation in vacuo, the residue was purified by FCC (dichloromethane). Recrystallization from dichloromethane/hexane gave pure **1** (1.0 mg, 25%); vis (CH$_2$Cl$_2$) λ_{max} = 637 (rel., 0.02), 586 (0.06), 563 (0.10), 521 (0.06), 418 nm (1.00); ^{1}H NMR (CDCl$_3$) δ = 10.15, 9.92, 9.87 (each 1H, s, *meso*-H × 3), 5.93 (2H, s, 13^2-CH$_2$), 4.35–3.94 (14H, m, β-CH$_2$ × 7), 2.09–1.78 (21H, m, β-CCH$_3$ × 7), −2.35, −3.28 (each 1H, s, NH × 2); MS (FAB) *m/z* 546.3 (M$^+$), calcd. for C$_{36}$H$_{42}$N$_4$O: 546.3.

2.2.5. Synthesis of 13^1-deoxo-porphyrin bearing the E-ring 3

To a 1,2-dichlorobenzene solution (30 ml) of 13-vinyl-**9** (53 mg), an excess amount of *p*-TsOH (2.0 g) was added and refluxed for 8 h under nitrogen [13]. After cooling, the reaction mixture was washed with aq. 4% NaHCO$_3$ and water, dried over Na$_2$SO$_4$, and evaporated to dryness. The residue was purified by FCC: starting material **9** (1:1 dichloromethane/hexane) and desired product **3** (1% diethyl ether/dichloromethane). Recrystallization from methanol gave pure **3** as a purple solid (23.4 mg, 43%); vis (CH$_2$Cl$_2$) λ_{max} = 616 (rel., 0.02), 564 (0.03), 535 (0.02), 500 (0.07), 400 nm (1.00); ^{1}H NMR (CDCl$_3$) δ = 10.07, 10.03, 9.99 (each 1H, s, *meso*-H × 3), 5.40 (2H, m, 13^1-CH$_2$), 4.19–4.13, 4.08, 4.03 (8H + 2H + 4H, m, β-CH$_2$ × 7), 4.12 (2H, m, 13-CH$_2$), 1.99, 1.96–1.87, 1.80 (3H + 15H + 3H, m, β-CCH$_3$ × 7), −2.96, −3.73 (each 1H, s, NH × 2); MS (FAB) *m/z* 532.2 (M$^+$), calcd. for C$_{36}$H$_{44}$N$_4$: 532.4.

2.2.6. Synthesis of zinc 13^1-oxoporphyrin bearing the E-ring Zn1

Zinc insertion of **1** was achieved according to standard procedure [20,26]. FCC separation (3–5% diethyl ether/dichloromethane) and recrystallization from dichloromethane/hexane to give pure **Zn1** as a red solid; vis (CH$_2$Cl$_2$) λ_{max} = 602 (rel., 0.14), 555 (0.05), 535 (0.04), 421 nm (1.00); ^{1}H NMR (CDCl$_3$) δ = 10.01, 9.69, 9.67 (each 1H, s, *meso*-H × 3), 5.92 (2H, s, 13^1-CH$_2$), 4.34, 4.02–3.93, 3.87 (2H + 10H + 2H, m, β-CH$_2$ × 7), 2.09, 1.89–1.83, 1.74 (3H + 15H + 3H, m, β-CCH$_3$ × 7); MS (FAB) *m/z* 608.0 (M$^+$), calcd. for C$_{36}$H$_{40}$N$_4$O^{64}Zn: 608.3.

2.2.7. Synthesis of zinc13^1-deoxo-porphyrin bearing the E-ring Zn3

Zinc insertion of **3** was performed similarly as in **1** → **Zn1**, followed by FCC separation (3–5% diethyl ether/dichloromethane) and recrystallization from dichloromethane/hexane to give pure **Zn3** as a red solid; vis (CH$_2$Cl$_2$) λ_{max} = 567

(rel., 0.04), 532 (0.04), 404 nm (1.00); ^{1}H NMR (CDCl$_3$) δ = 10.00, 9.94, 9.91 (each 1H, s, *meso*-H × 3), 5.46 (2H, m, 13^1-CH$_2$), 4.00–4.18 (2H, m, 13-CH$_2$), 4.26–4.18, 4.15–3.99 (2H + 12H, m, β-CH$_2$ × 7), 2.03, 1.94–1.86, 1.78 (3H + 15H + 3H, m, β-CCH$_3$ × 7); MS (FAB) *m/z* 594.2 (M$^+$), calcd. for C$_{36}$H$_{42}$N$_4$^{64}Zn: 594.3.

3. Results and discussion

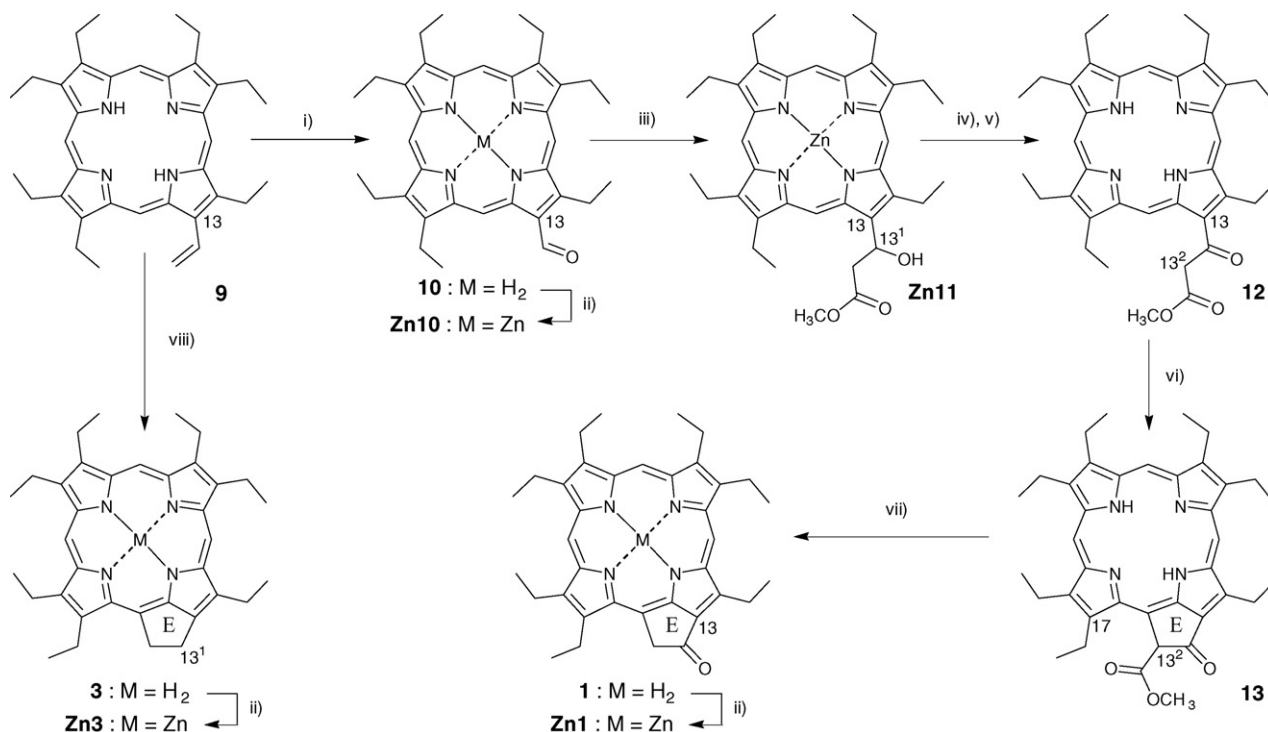### 3.1. Synthesis of porphyrins (Zn)1/3 bearing the E-ring and (Zn)2/4 lacking it

Synthesis of 13^1-oxo-**1** bearing the E-ring was achieved as in Scheme 2. Indium-mediated alkylation [24] of the metal-free **10** [20] produced indium complex of **11** due to an unfavorable insertion of indium to the cyclic tetrapyrrole. Demetallation of the central indium was so difficult that zinc was preliminarily metallated to avoid the unfavorable indium insertion. The indium-mediated reaction of zinc 13-formyl-porphyrin **Zn10** with methyl bromoacetate followed by its FCC separation gave zinc 13-[1-hydroxy-2-(methoxycarbonyl)ethyl]porphyrin **Zn11** in 20% yield. Since **Zn10** was recovered on FCC, the conversion yield reached 40% after reactions repeated 4 times. Oxidation [20,25] of the 13^1-hydroxy group in **Zn11** and successive zinc demetallation [21] gave 13-[2-(methoxycarbonyl)acetyl]porphyrin **12**. Photocyclization of **12** succeeded in a similar manner to the previous report by Smith and co-workers [8] to give porphyrin **13** possessing a methoxycarbonyl group on the exo-five-membered E-ring. The methoxycarbonyl group in **13** was removed by refluxing the collidine solution [22] to give desired porphyrin **1** possessing 13-keto-carbonyl group fixed on the E-ring, similar to natural (B)Chls.

13^1-Deoxo-**3** was prepared from **9** in a similar manner to the previous report [13]. 13-Acetyl-porphyrin **2** was synthesized according to the previous report [20]. Zinc metallations of all the above synthetic porphyrins **1–3** and commercially available **4** quantitatively proceeded to give the corresponding **Zn1**–**Zn4**. Molecular structures of all the synthetic compounds were determined by their 1D ^{1}H and 2D ^{1}H–^{1}H COSY and NOESY and FAB–MS spectra.

3.2. ^{1}H NMR spectra of synthetic porphyrins 12 and 13 possessing a β-keto-ester moiety

The 13^2-methoxycarbonyl group of synthetic porphyrins **12** and **13** is situated at the α-position of the 13-keto-carbonyl group, giving a β-keto-ester. Both porphyrins **12** and **13** having a β-keto-ester without and with fixation of the E-ring, respectively, are suitable for observing the structural effect of the E-ring on its keto–enol tautomerism. It is noteworthy that the enol species of natural chlorophyllous pigments possessing the E-ring could not be detected in their organic solutions under ambient neutral conditions (on NMR and IR spectroscopies) [27].

Fig. 3 shows partial ^{1}H NMR spectra of synthetic metal-free porphyrins **12** and **13** having four and three *meso*-protons, respectively, in the low field region. ^{1}H NMR spectrum of **13**

Scheme 2. Synthesis of 13^1-oxo/deoxo-porphyrins **1/3** bearing the E-ring. (i) OsO$_4$, NaIO$_4$, THF–1,4-dioxane–H$_2$O; (ii) Zn(OAc)$_2$, CH$_2$Cl$_2$–CH$_3$OH; (iii) BrCH$_2$COOCH$_3$, indium powder, THF, then ultrasound; (iv) N-methylmorpholine N-oxide, nPr$_4$NRuO$_4$, CH$_2$Cl$_2$; (v) 10% HCl aq., THF; (vi) Tl(OCOCF$_3$)$_3$, CH$_2$Cl$_2$, $h\nu$; (vii) collidine, reflux; (viii) p-TsOH, 1,2-dichlorobenzene, reflux.

bearing the E-ring shows three *meso*-peaks while that of **12** lacking the E-ring has eight *meso*-peaks accompanied with a specific proton signal at 13.24 ppm. The eight protons were categorized into two sets of four *meso*-protons by their integral ratio and ^{1}H–^{1}H NOESY spectra, of which one *meso*-peak in a set had a NOE correlation with a CH$_2$-proton signal at 4.76 ppm, being traced to the keto-form (C15H–C14–C13–C13^1(=O)–C13$^2H_2$, correlation between C15H and C13$^2H_2$). In contrast, one *meso*-peak in the other set had a NOE correlation with a CH-signal situated at a lower field (6.12 ppm), indicating the enol-form (C15H–C14–C13–C13^1(OH)=C13^2H, correlation

Fig. 3. ^{1}H NMR spectra of **12** (lower) and **13** (upper) in CDCl$_3$. K and E indicate proton-peaks of keto- and enol-forms, respectively.

between C15H and C13^2H). The lowest field shifted proton signal of the latter was characteristic of enol-13^1-OH. Therefore, **12** lacking the E-ring was comprised of both the keto- and enol-forms in a CDCl$_3$ solution at room temperature. Each proton signal of **12** in CDCl$_3$ was assigned by its ^{1}H–^{1}H NOESY spectrum; keto:enol ratio of **12** in CDCl$_3$ was estimated as 5:6 from the integral ratio of its ^{1}H NMR peaks. In contrast, synthetic porphyrin **13** bearing the E-ring showed no enol-species in its ^{1}H NMR spectrum, indicating that a porphyrin bearing the E-ring favored the keto-form as in natural (B)Chls (vide supra).

Energetically minimized molecular structures of keto/enol-**12** and **13** were obtained by successive MM+ and PM3 calculations [28,29]; total energies of keto/enol-**12** were 278/299 kJ/mol and those of keto/enol-**13** were 298/370 kJ/mol, respectively. The large difference in energy between the keto and enol forms of **13** is consistent with the exclusive formation of keto-**13** in the solution. The energetically minimized enol-**12** (left drawing in Fig. 4) shows little distortion in its porphyrin π-system while that of enol-**13** (right in Fig. 4) was more distorted by a steric repulsion between the 13^2-methoxycarbonyl and its neighboring 17-ethyl groups as indicated by arrows on the lower side view of Fig. 4. Standard deviations of 20 carbons and 4 nitrogens on the porphyrin macrocycle of keto/enol-**12** and -**13** from their mean planes were calculated as in 0.033/0.095 and 0.030/0.150 Å, respectively. Such a distortion also agrees with the experimental results. The presence of the E-ring on cyclic tetrapyrroles suppressed the keto-to-enol tautomerism to give predominantly the keto-form in **13**.
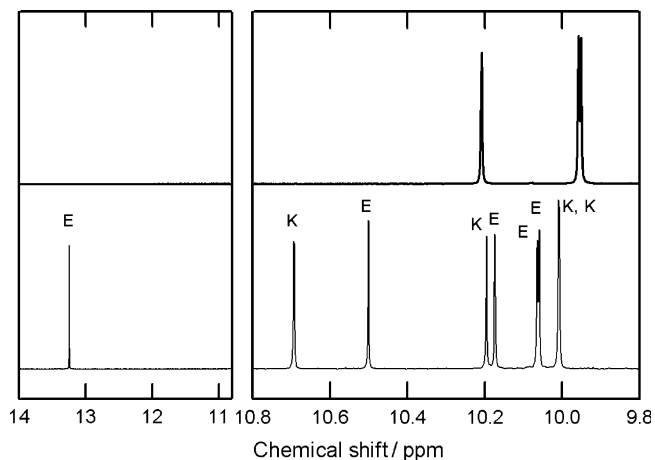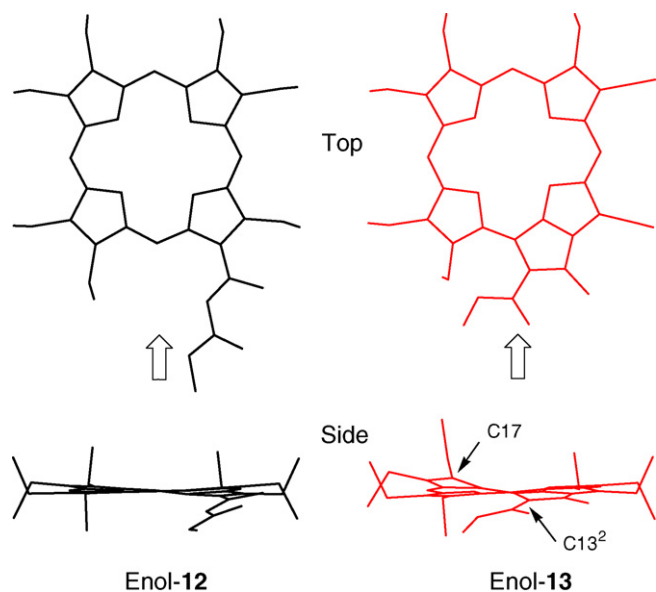
Fig. 4. Energetically minimized molecular structures of enol-**12** (left) and enol-**13** (right) obtained by MM+/PM3 calculations (hydrogen atoms are omitted). The side views (lower) are the view from the arrow in the upper drawings.

3.3. Visible absorption and fluorescence spectra of metal-free porphyrins 1–4 and their zinc complexes Zn1–Zn4

The visible absorption spectrum of a metal-free porphyrin is comprised of intense Soret (around 400 nm) and four Q-bands (500–650 nm, called QIV, QIII, QII and QI in going from blue to red regions) [30]. Positions and intensities of each Q-band are sensitive to the peripheral substituents at the β-position (2,3,7,8,12,13,17,18-positions); a porphyrin possessing no electron-withdrawing group at the β-position has intensities of Q-bands in the order of QIV > QIII > QII > QI (etio-type), and introduction of one or two electron-withdrawing group(s) (e.g., a carbonyl group) at the β-position(s) causes red-shifts in absorption maxima of the Q-bands with a different order in the intensities of QIII > QIV > QII > QI or QIII > QII > QIV > QI (rhodo- or oxorhodo-type). Visible absorption spectra of metalloporphyrins (Zn, Ni, Mg, etc.) have red-shifted Soret bands, compared with their corresponding metal-free porphyrins, and two Q bands (Qβ and Qα formed by degenerations of QIV/QII and QIII/QI, respectively) in the region from 500 to 600 nm due to an increase of structural symmetry of the π-system ($C_2 \rightarrow C_4$).

Compared with Soret and Q-bands of metal-free **4** in dichloromethane (etio-type, broken line in Fig. 5B), both metal-free 13^1-oxo-**1** and **2** in the solution (rhodo- and oxorhodo-types, solid and broken lines in Fig. 5A) showed red-shifted absorption maxima as expected. Obvious spectral differences were observed in **1** and **2** having the same electron-withdrawing 13-carbonyl group (13^1-oxo); **1** bearing the E-ring gave more red-shifted absorption peaks than did **2** lacking it. A similar observation was obtained in their zinc complexes (see solid and broken lines in Fig. 5C for **Zn1** and **Zn2**, respectively). To elucidate these spectral differences, the following two factors are separately discussed: (1) formation of the exo-five-membered
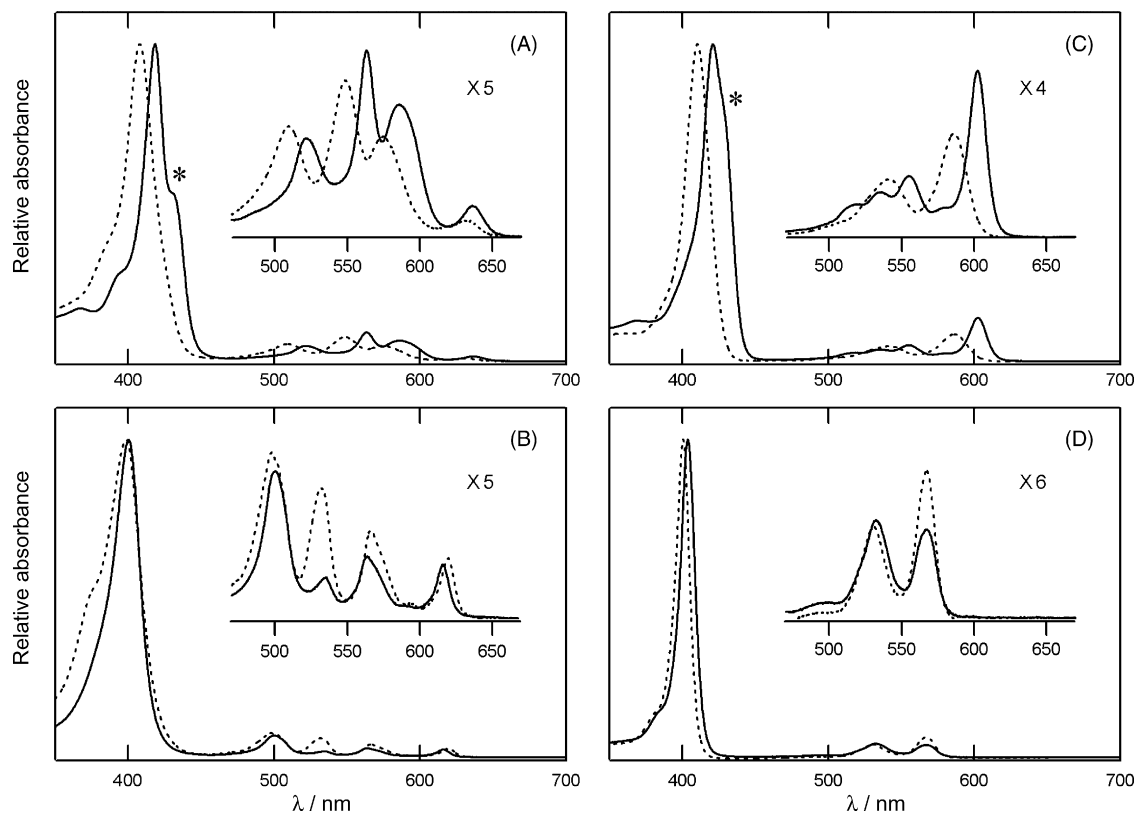

Fig. 5. Visible absorption spectra of synthetic metal-free **1–4** (left) and the corresponding zinc complexes (**Zn1–4**, right) in dichloromethane. The top (A/C) and bottom drawings (B/D) are **1·2/Zn1·2** and **3·4/Zn3·4**, respectively. Synthetic porphyrins bearing the E-ring (**Zn**)**1/3** and lacking it (**Zn**)**2/4** are drawn in solid and broken lines, respectively. The spectra were normalized at the Soret absorption maxima.
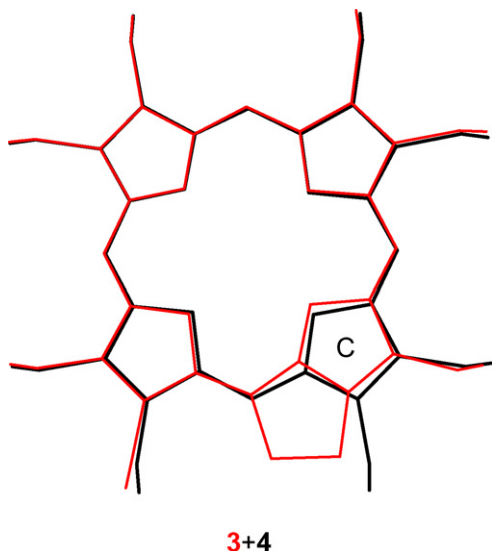
Fig. 6. Energetically minimized molecular structures of **3** and **4** (red and black drawings).

E-ring distorted the geometries of four pyrrole units, and (2) the keto-carbonyl group was fixed on the porphyrin π-plane to be coplanar.

3.3.1. Effect of the E-ring; comparison between visible absorption and fluorescence emission spectra of (Zn)3 and (Zn)4

First, we discuss the effect of formation of the exo-five-membered E-ring by visible absorption spectral analyses between 13^1-deoxo-**3** and **4**, whose molecular structures were favorable to investigate the effect of sole formation of the E-ring without considering any other substituent effects. Synthetic 13^1-deoxo-porphyrins **3** and **4** bearing and lacking the E-ring have no electron-withdrawing substituents at the peripheral β-positions, and their molecular structures are distinguished only in the presence or absence of the exo-five-membered E-ring. The formation of the E-ring in **3** caused altered geometries of the location of four pyrrole units. Energetically minimized molecular structures of **3** and **4** obtained by MM+/PM3 calculation [28,29] revealed that a distortion derived from the formation of the E-ring in **3** altered the geometry of tetrapyrrolic macrocycle, and especially, the C-ring in **3** rotated by 5–7° in a clockwise direction, compared with that in **4** (see Fig. 6). Synthetic **3** bearing the E-ring thus had a slightly asymmetrical π-system, which should change the optical properties.

As expected, visible absorption spectra of metal-free **3** and **4** (solid and broken lines in Fig. 5B) showed slightly different absorption maxima within 3 nm (see Table 1). A slightly sharper Soret band was observed in **3** than in **4**. The Q-band intensities in **4** having no electron-withdrawing groups were etio-type (QIV > QIII > QII > QI) as described above, while those in **3** were another type (QIV > QII > QI > QIII).[1] Soret, QIV and QIII

---

[1] The Q-band intensities in **3** were similar to those in the previously reported analog, 13^2,15-cycloporphyrin (**6**, Scheme 1) [9]: vis (CHCl₃) λ_{max} (log ε) = 616 (3.79), 563 (3.81), 534 (3.61), 500 (4.20), 400 nm (5.36).

Table 1
Electronic absorption and emission maxima (nm) of metal-free **1**–**4**, **14** and **15** in dichloromethane

Compound	Absorption					Emission	
	Soret	QIV	QIII	QII	QI	QI′	QII′
1	418.2	521.2	563.2	586.0	636.6	640.2	703.6
2	407.8	509.6	548.6	574.8	632.4	636.4	690.2
3	400.4	500.0	534.8	563.6	616.0	616.8	679.0
4	398.6	497.8	531.4	565.8	619.4	620.2	684.2
14	418.6	524.2	566.6	590.0	640.0	644.6	708.6
15	406.6	512.0	552.2	576.0	638.6	639.0	696.0

bands in the visible absorption spectrum of **3** were relatively red-shifted compared to those in **4** while the energetically lower QII and QI bands were blue-shifted. Fluorescence emission spectra of metal-free **3** and **4** showed similar spectral shapes with a small Stokes shift of 0.8 nm, respectively (thin solid and broken lines in Fig. 7A; Table 1). Small and broadened emissions were also observed at a longer wavelength region than the intense QI′ emission.

Zinc complexes **Zn3** and **Zn4** were examined by visible absorption spectroscopy and showed similar results (solid and broken lines in Fig. 5D) as in their metal-free **3/4**. Their relative
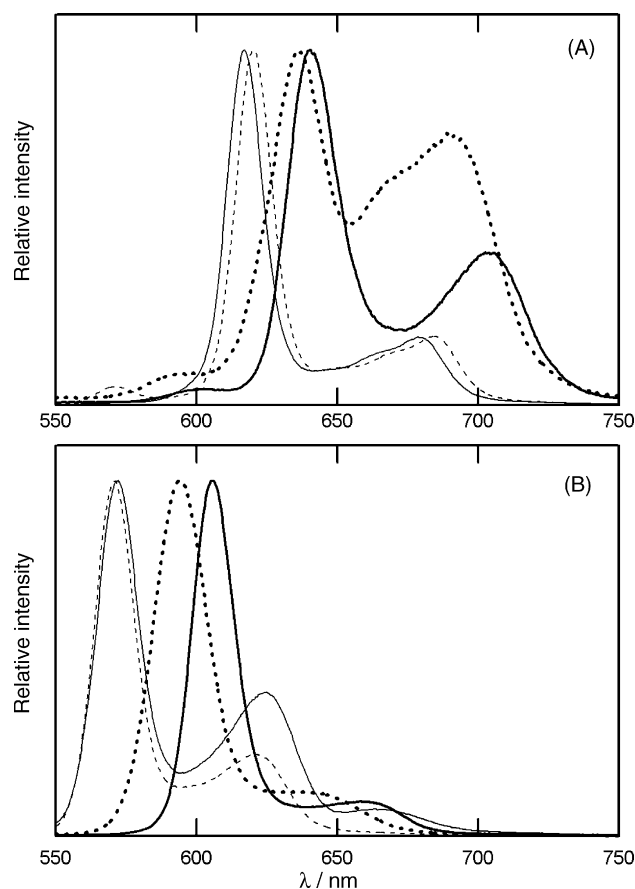

Fig. 7. Fluorescence emission spectra of metal-free (A) and zinc porphyrins (B). The spectra of (**Zn**)**1**, (**Zn**)**2**, (**Zn**)**3** and (**Zn**)**4** were depicted by solid, broken, thin solid and thin broken lines, respectively. All the spectra were obtained by excitation at the Soret absorption maxima, and normalized at the intense peaks.

intensity of Qα/Qβ in **Zn3** (0.9) was smaller than that in **Zn4** (1.6), which was ascribable to the less intense QIII band in metal-free **3**: combination of QI with QIII corresponds to Qα and that of QII with QIV to Qβ. Their absorption maxima including their Soret bands were slightly different within 3 nm (see Table 1). As compared to **Zn4**, Soret and Qβ bands in **Zn3** were relatively shifted to a longer wavelength region while the energetically lowest Qα band showed no shift. Fluorescence emission spectra of **Zn3/Zn4** showed two bands, Qα′ and Qβ′ bands at shorter and longer wavelength regions, respectively (thin solid and broken lines in Fig. 7B). The relative intensity of Int(Qα′)/Int(Qβ′) in **Zn3** (2.5) was less than that in **Zn4** (4.4), which is consistent with the ratio of Qα/Qβ absorption peak intensities in **Zn3** (0.90) and **Zn4** (1.6).

As compared with (**Zn**)**4** lacking the E-ring, small red-shifts in the Soret and QIV/QIII or Qβ bands were observed in (**Zn**)**3**, but the difference between visible absorption maxima of 13^1-deoxo-**3** and **4** was so small that the large difference obtained between those of 13^1-oxo-**1** and **2** could not be explained solely by E-ring formation.

3.3.2. Effect of conformationally fixed or flexible 13^1-oxo-group; comparison between visible absorption and fluorescence emission spectra of (Zn)1 and (Zn)2

As compared to the visible absorption spectrum of metal-free 13^1-oxo-**2** lacking the E-ring (broken line in Fig. 5A), that of metal-free 13^1-oxo-**1** bearing the E-ring (solid line in Fig. 5A) showed red-shifted absorption bands and an obvious shoulder peak at a longer wavelength of the Soret band (* mark in Fig. 5A). Soret, QIV, QIII and QII absorption maxima of **1** were shifted to 10–15 nm longer wavelengths than those of **2**, while the energetically lowest QI band showed a relatively small red-shift (4 nm for **2** → **1**). Since spectral change by the presence or absence of the E-ring was relatively small as described above, the difference between visible absorption spectra of **1** and **2** must be derived from the electronic effect of the conformationally fixed and flexible 13^1-oxo groups.

The pattern in Q-band intensities of **1** was an oxorhodo-type and that of **2** was a rhodo-type. As in **3** and **4**, the cyclization between 13- and 15-positions (**1** → **2**) also altered the relative intensities of the Q-bands. In visible absorption spectra of 13^1-deoxo-**3/4**, a decrease of QIII-band intensity was observed by the formation of the E-ring but such a suppression was not obtained in 13^1-oxo-**2** → 13^1-oxo-**1**, which is probably due to the electronic effect of the larger conjugated 13^1-oxo group in **1**.

Fluorescence emission spectra of **1** and **2** in dichloromethane (thick solid and broken lines in Fig. 7A) showed a major peak with a 4-nm Stokes shift and minor bands at the longer wavelength region which were relatively more intense than those of **3** and **4**. Such a difference between **1/2** and **3/4** would be ascribable to the electron-withdrawing effect of their 13^1-oxo groups. Fluorescence emission maximum of **1** was shifted to a longer wavelength region than that of **2**, similar to their visible absorption maxima.

Zinc complexes 13^1-oxo-**Zn1/Zn2** (bearing/lacking the E-ring) were examined by visible absorption spectroscopy (solid/broken lines in Fig. 5C). As observed in the difference
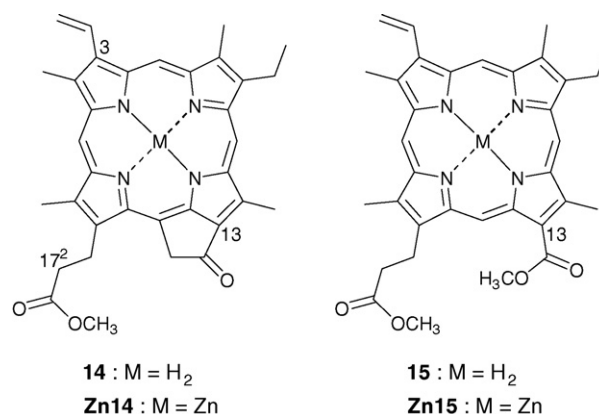

Fig. 8. Molecular structures of semi-natural 13^1-oxo-porphyrins bearing the E-ring (**Zn**)**14** and lacking it (**Zn**)**15**.

between their metal-free **1** and **2**, visible absorption spectrum of 13^1-oxo-**Zn1** bearing the E-ring showed red-shifted Soret and two major Q-bands, compared with those of **Zn2** lacking it, and a shoulder peak at the longer wavelength of the Soret band (* in Fig. 5C) was observed. Moreover, **Zn1** gave at least three peaks in the region of Q-band, which were ascribable to the effect of the fixed carbonyl group in **Zn1**, because such obvious side bands could not be observed in visible absorption spectra of 13^1-oxo-**Zn2** lacking the E-ring and also 13^1-deoxo-**Zn3** bearing it. The relative intensity of Qα band in **Zn1** (0.14) was enlarged with a smaller FWHM (400 cm^{-1}), compared with those of **Zn2** (0.09, 660 cm^{-1}). Fluorescence emission spectra of **Zn1** and **Zn2** (thick solid and broken lines in Fig. 7B) showed similar spectral shapes and the peaks of **Zn1** were red-shifted compared to those of **Zn2**.

In addition to the simple comparison of synthetic (**Zn**)**1** with (**Zn**)**2**, we demonstrated the spectral differences between semi-natural porphyrins (**Zn**)**14** and (**Zn**)**15** (see their molecular structures drawn in Fig. 8). Both **14** and **15** were prepared from naturally occurring Chl-*a*, so that their peripheral substituents were similar to natural (B)Chls. Porphyrin (**Zn**)**14** bearing the E-ring has vinyl and methoxycarbonyl groups at the 3- and 17^2-positions, and (**Zn**)**15** lacking the E-ring has a methoxycarbonyl group at the 13-position instead of the acetyl group in (**Zn**)**2**. Despite numerous different peripheral substituents, visible absorption and fluorescence spectra of (**Zn**)**14** and (**Zn**)**15** (see absorption and emission maxima drawn in Tables 1 and 2) showed similar differences as in (**Zn**)**1** and (**Zn**)**2**, indicating

Table 2
Electronic absorption and emission maxima (nm) of **Zn1**–**Zn4**, **Zn14** and **Zn15** in dichloromethane

Compound	Absorption			Emission	
	Soret	Qβ	Qα	Qα′	Qβ′
Zn1	420.8	555.0	602.4	605.4	–
Zn2	410.2	541.2	586.0	594.2	–
Zn3	403.8	532.2	567.2	572.0	624.4
Zn4	400.6	530.6	567.2	570.8	621.2
Zn14	423.8	560.4	609.8	613.6	–
Zn15	412.0	547.0	591.6	596.6	–

that the fixation of carbonyl group on the E-ring would control their π-conjugate systems as well as their optical properties.[2]

The flexible carbonyl group as in (**Zn**)**2** or (**Zn**)**15** can rotate the C13–C13^1 bond, having various configurations (rotamers). The structural variation would decrease the electron-withdrawing factor (red-shifts in absorption peaks). The situation of the 13^1-oxo group also affected their absorption and emission spectral shapes; the spectral shape of **1** was comprised of some distinct bands including the shoulder peak (* mark in Fig. 5A) while that of **2** was broadened throughout. Ultraviolet absorption spectra of acetophenone and 1-indanone, which are one of the simplified models possessing flexible or fixed carbonyl group on the aromatic π-system, showed that conformationally fixed carbonyl group in 1-indanone induced red-shifted absorption bands with an appearance of a shoulder peak at the longer wavelength: absorption maxima of acetophenone and 1-indanone were observed at 241 and 242/248(sh) nm in dichloromethane and also reported to be 238 and 239/244(sh) nm in heptane [31]. These are similar to the present differences between (**Zn**)**1** and (**Zn**)**2**: red-shifts in absorption bands with the appearance of a shoulder peak in (**Zn**)**2** → (**Zn**)**1**. Inoue and his colleagues suggested that the E-ring in chlorophylls led to red-shifted and enlarged absorption bands from molecular orbital calculations [32]. We could experimentally confirm their suggestion by optical spectral comparison among simply and systematically prepared models **1**–**4**.

4. Concluding remarks

A series of 13^1-oxo/deoxo-porphyrins bearing/lacking an exo-five-membered E-ring was examined by their visible absorption and fluorescence emission spectra. Spectral differences between 13^1-deoxo-(**Zn**)**3** bearing the E-ring and (**Zn**)**4** lacking it were relatively small, indicating that just introduction of the E-ring little affected optical properties. In contrast, visible absorption spectra of 13^1-oxo-(**Zn**)**1** bearing the E-ring and (**Zn**)**2** lacking it showed obvious differences: absorption and emission bands in **1** were shifted to a longer wavelength region than in **2**. These results indicated that conformational fixation of 13^1-oxo group in **1** strongly affected the optical properties of porphyrinoids. The E-ring in naturally occurring chlorophyllous pigments have already been reported to be structurally required in their complexes with peptides [5,33]; the conformationally fixed 13-carbonyl group is important for robust interaction with protein scaffolds, which is responsible for various functions including efficient and rapid energy- and electron-transfer in photosynthesis. In this paper we demonstrated that the presence of the E-ring in porphyrinoids suppressed their keto-to-enol tautomerism to fix the keto-form, which was appropriate for the above intramolecular interactions. Furthermore, in the visible

absorption spectrum of **Zn1**, relative intensity of the energetically lowest Qα band was enlarged by the presence of the E-ring. In the natural photosynthetic systems, sunlight is harvested in their antenna systems, followed by singlet excited energy transfer to the reaction centers, where energetically lowest absorption and emission bands in (bacterio)chlorin chromophores function in significant roles. The fixation of 13^1-oxo group on the E-ring leading to enlargement of the energetically lowest absorption band is apparently suitable and necessary for the photosynthetic cyclic tetrapyrroles.

References

[1] H. Scheer, in: B.R. Green, W.W. Parson (Eds.), Light-Harvesting Antennas in Photosynthesis, Kluwer Academic Publishers, Dordrecht, 2003, pp. 29–81.
[2] R.D. Willows, Nat. Prod. Rep. 20 (2003) 327–341.
[3] H.J. Callot, R. Ocampo, in: K.M. Kadish, K.M. Smith, R. Guilard (Eds.), Porphyrin Handbook, Academic Press, San Diego, 2000, pp. 349–398.
[4] T. Miyatake, H. Tamiaki, J. Photochem. Photobiol., C: Photochem. Rev. 6 (2005) 89–107.
[5] T. Oba, H. Tamiaki, Bioorg. Med. Chem. 13 (2005) 5733–5739.
[6] T.S. Balaban, H. Tamiaki, A.R. Holzwarth, in: F. Würthner (Ed.), Supramolecular Dye Chemistry, Springer–Verlag, Heidelberg, 2005, pp. 1–38.
[7] E.W. Baker, A.H. Corwin, E. Klesper, P.E. Wei, J. Org. Chem. 33 (1968) 3144–3148.
[8] G.W. Kenner, S.W. McCombie, K.M. Smith, J. Chem. Soc., Perkin Trans. 1 (1974) 527–530.
[9] I.A. Chaudhry, P.S. Clezy, A.H. Mirza, Aust. J. Chem. 33 (1980) 1095–1104.
[10] K.M. Smith, K.C. Langry, O.M. Minnetian, J. Org. Chem. 49 (1984) 4602–4609.
[11] P.S. Clezy, J.K. Prashar, Aust. J. Chem. 43 (1990) 825–837.
[12] P.S. Clezy, U. Jenie, J.K. Prashar, Aust. J. Chem. 43 (1990) 839–856.
[13] C. Bauder, R. Ocampo, H.J. Callot, Tetrahedron 48 (1992) 5135–5150.
[14] C. Jeandon, R. Ocampo, H.J. Callot, Tetrahedron Lett. 34 (1993) 1791–1794.
[15] T.D. Lash, D.M. Quizon-Colquitt, C.M. Shiner, T.H. Nguyen, Z. Hu, Energy Fuels 7 (1993) 172–178.
[16] W. Li, T.D. Lash, Tetrahedron Lett. 39 (1998) 8571–8574.
[17] J.A. Bastian, T.D. Lash, Tetrahedron 54 (1998) 6299–6310.
[18] B. Zhang, T.D. Lash, Tetrahedron Lett. 44 (2003) 7253–7256.
[19] P.H. Hynninen, in: H. Scheer (Ed.), Chlorophylls, CRC Press, Boca Raton, 1991, pp. 145–209.
[20] H. Tamiaki, S. Kimura, T. Kimura, Tetrahedron 59 (2003) 7423–7435.
[21] H. Tamiaki, T. Watanabe, T. Miyatake, J. Porphyrins Phthalocyanines 3 (1999) 45–52.
[22] G.W. Kenner, S.W. McCombie, K.M. Smith, J. Chem. Soc., Perkin Trans. 1 (1973) 2517–2523.

---

[2] Similar difference (red-shifts in absorption bands) was also observed in visible spectra of 17,18-dihydro-**14** and **15**; 17*S*,18*S*-dihydro-**14**: vis (CH$_2$Cl$_2$) $\lambda_{max} = 667$ (rel., 0.43), 610 (0.07), 539 (0.09), 509 (0.10), 414 nm (1.00); 17*S*,18*S*-dihydro-**15**: vis (CH$_2$Cl$_2$) $\lambda_{max} = 666$ (rel., 0.36), 609 (0.04), 529 (0.03), 499 (0.08), 402 nm (1.00). Optical properties of chlorin π-system are also affected by the formation of the E-ring.

[23] K.M. Smith, D.J. Simpson, J. Chem. Soc., Chem. Commun. (1987) 613–614.

[24] S. Yagai, H. Tamiaki, J. Chem. Soc., Perkin Trans. 1 (2001) 3135–3144.

[25] S.V. Ley, J. Norman, W.P. Griffith, S.P. Marsden, Synthesis (1994) 639–666.

[26] H. Tamiaki, M. Amakawa, Y. Shimono, R. Tanikaga, A.R. Holzwarth, K. Schaffner, Photochem. Photobiol. 63 (1996) 92–99.

[27] A.N. Kozyrev, T.J. Dougherty, R.K. Pandey, Chem. Commun. (1998) 481–482.

[28] Y. Kureishi, H. Tamiaki, J. Porphyrins Phthalocyanines 2 (1998) 159–169.

[29] M. Kunieda, H. Tamiaki, J. Org. Chem. 70 (2005) 820–828.

[30] K.M. Smith, in: K.M. Smith (Ed.), Porphyrins and Metalloporphyrins, Elsevier Scientific Publishing Company, Amsterdam, 1975, pp. 3–28.

[31] G.D. Hedden, W.G. Brown, J. Am. Chem. Soc. 75 (1953) 3744–3748.

[32] Y. Nonomura, S. Igarashi, N. Yoshioka, H. Inoue, Chem. Phys. 220 (1997) 155–166.

[33] B. Loll, J. Kern, W. Saenger, A. Zouni, J. Biesiadka, Nature 438 (2005) 1040–1044.